*International Journal of Neuropsychopharmacology* (2014), **17**, 235–246. © CINP 2013
doi:10.1017/S1461145713000850

ARTICLE

# The JNK inhibitor, SP600125, potentiates the glial response and cell death induced by methamphetamine in the mouse striatum

**Andres Urrutia[1,2]*, Noelia Granado[1,2]*, Maria Dolores Gutierrez-Lopez[1,2], Rosario Moratalla[3], Esther O'Shea[1,2] and Maria Isabel Colado[1,2]**

[1] *Departamento de Farmacologia, Facultad de Medicina, Universidad Complutense, Madrid, Spain*
[2] *Instituto de Investigación Sanitaria del Hospital Clínico San Carlos (IdISSC), Madrid, Spain*
[3] *Instituto Cajal, Consejo Superior de Investigaciones Científicas, CSIC, Madrid, Spain*

**Abstract**

This study investigates the effect of the selective Jun $NH_2$-terminal kinase 1/2 (JNK1/2) inhibitor, (SP600125) on the striatal dopamine nerve terminal loss and on the increased interleukin-15 (IL-15) expression and glial response induced by methamphetamine (METH). Mice were given repeated low doses of METH (4 mg/kg, i.p., three times separated by 3 h) and killed 24 h or 7 d after the last dose. SP600125 (30 mg/kg, i.p) was administered 30 min before the last METH injection. Results indicate that METH produced dopaminergic axonal neurotoxicity reflected as a marked decrease in the striatal density of tyrosine hydroxylase-immunoreactive (TH-ir) fibres and dopamine transporter-immunoreactivity (DAT-ir) 24 h after dosing. These effects were not modified by SP600125. This compound also failed to prevent the long-term loss of dopamine levels and DAT observed 7 d following METH injection. Nevertheless, SP600125 potentiated METH-induced striatal cell loss reflected by an increase in Fluoro-Jade immunostaining, cleaved capase-3 immunoreactivity and the number of terminal deoxyncleotidyl transferase-mediated dUTP nick end labelling (TUNEL) positive cells. In line with a deleterious effect of JNK1/2 inhibition, SP600125 increased the astroglial and microglial response induced by METH and interfered with drug-induced IL-15 expression. Together these data indicate that, not only does SP600125 fail to protect against the dopaminergic damage induced by METH but also, in fact, it potentiates the glial response and the non-dopaminergic striatal cell loss caused by the drug.

*Received 26 March 2013; Reviewed 9 April 2013; Revised 28 June 2013; Accepted 2 July 2013; First published online 8 October 2013*

**Key words:** Caspase-3, glia, IL-15, JNK, methamphetamine.

## Introduction

Methamphetamine (METH) is a powerful psychostimulant with high abuse potential (UNODC, 2012). In mice, repeated administration of METH produces dopaminergic neurodegeneration consisting in the loss of axons and terminals in the striatum and of cell bodies in the substantia nigra (Hirata and Cadet, 1997; Krasnova and Cadet, 2009; Granado et al., 2010). Numerous studies have shown a long-term substantial decrease in the concentration of dopamine and its metabolites, a loss in the density of plasmalemmal and vesicular dopamine transporters and a decrease in tyrosine hydroxylase activity (Sonsalla et al., 1989; O'Callaghan and Miller, 1994; Hogan et al., 2000; Itzhak et al., 2000; Ares-Santos et al., 2012). In addition, METH administration induces reactive astrocytosis and microgliosis and increases interleukin-15 (IL-15) expression (Thomas et al., 2004b, 2008; Granado et al., 2011a, b).

The mechanisms underlying this toxicity are still unknown but it appears that several factors are involved including; oxidative stress, neuroinflammatory processes, hyperthermia and mitochondrial/endoplasmic reticulum stress (Itzhak et al., 1998, 2000; Deng and Cadet, 1999; Imam et al., 2001; Krasnova and Cadet, 2009).

We have recently shown that repeated administration of low-dose METH disrupts the integrity of the blood-brain barrier (BBB) (Urrutia et al., 2013). Thus, shortly after METH treatment there is a reduction in striatal laminin expression and increased immunoglobulin (IgG) immunoreactivity colocalizing with areas of greater matrix metallopeptidase-9 (MMP-9) activity. Administration of the JNK1/2 inhibitor, SP600125, prevented all these changes and attenuated the increased expression of p-JNK1/2 induced by the drug (Urrutia et al., 2013). In addition, METH generates a differential regulation of endothelial (ABC) transporters, which is controlled by apolioprotion-E (ApoE), most probably through its

Address for correspondence: Professor M. I. Colado, Departamento de Farmacologia, Facultad de Medicina, Universidad Complutense, Madrid 28040, Spain.
*Tel*: +91 394 1213 *Fax*: +91 394 1463 *Email:* colado@med.ucm.es
* These authors contributed equally to this study.

receptor ApoER2 that deactivates the JNK1/2/c-Jun pathway in brain endothelial cells (ElAli et al., 2012). Together, these data indicate that METH induces significant changes in BBB structure and function through the JNK pathway.

It is well known that JNK is linked to parenchymal stress and it has been associated with dopaminergic neurotoxicity in experimental models of Parkinson's disease (Saporito et al., 1999; Hunot et al., 2004; Wang et al., 2004) as well as cellular damage in a wide variety of experimental models such as ischaemic stroke (Borsello et al., 2003), spinal cord injury (Repici et al., 2012) and Alzheimer's disease (Morishima et al., 2001) among others, thus becoming a promising target for the treatment of neurodegenerative diseases.

The role of JNK signalling in *in vivo* METH-induced neuronal damage has been scarcely investigated with only one study showing that a single high dose of METH induces extensive apoptosis in the mouse brain, which is less evident in c-Jun knockout mice. METH-induced caspase-3 activity and Poly (ADP-ribose) polymerase (PARP) cleavage were also reduced in c-Jun heterozygous knockout mice (Deng et al., 2002).

The present study was undertaken to determine: (1) the ability of the selective JNK1/2 inhibitor SP600125 to prevent the striatal loss of dopamine nerve terminals induced by METH by assessing tyrosine hydroxylase (TH) and dopamine transporter (DAT) expression and dopamine concentration; (2) the role of SP600125 in the METH-induced striatal cell loss evaluated by counting Fluoro-Jade and terminal deoxyncleotidyl transferase-mediated dUTP nick end labelling (TUNEL) positive cells as well as expression of cleaved caspase-3; and (3) the effect of SP600125 on the METH-induced IL-15 expression and microglial and astroglial response by determining Iba-1 and glial fibrillary acidic protein antibody (GFAP) immunoreactivity in striatum.

## Materials and method

### *Animals and drug administration*

Adult male C57BL/6J mice (25–30 g, Harlan Laboratories Models, Barcelona) were used. Animals were housed in groups of 4–6 in conditions of constant temperature (21 °C ± 2 °C) in a 12 h light/dark cycle (lights on: 08 h 00 min) and given free access to food and water.

Mice received a neurotoxic regimen of three injections of (+)-METH (4 mg/kg, i.p.) at 3 h intervals and were killed 24 h or 7 d after drug dosing. Doses and protocol of administration were previously shown to produce a marked depletion of mouse striatal dopamine (Sanchez et al., 2003; Granado et al., 2010, 2011a; Ares-Santos et al., 2012). The time-points were chosen since METH produces an early loss of several dopaminergic parameters at 24 h, a time-point that is also suitable for glial determination. Seven days after METH a marked depletion of dopamine and dopamine transporters sites is observed and is commonly used as a time-point for assessing neurotoxicity (Sanchez et al., 2003; Granado et al., 2011a; Ares-Santos et al., 2012). METH hydrochloride (Sigma-Aldrich, USA) was dissolved in 0.9% w/v NaCl (saline) and injected in a volume of 10 ml/kg. The JNK inhibitor SP600125 (30 mg/kg, i.p.) was administered 30 min before the last METH injection and was dissolved in 20% DMSO in saline solution (Urrutia et al., 2013).

All experimental procedures were performed in accordance with the guidelines of the Animal Welfare Committee of the Universidad Complutense of Madrid (following European Council Directives 86/609/CEE and 2003/65/CE).

### *Measurement of monoamines and metabolites in striatum*

Seven d after treatment, the mice were killed by cervical dislocation and decapitation, the brains were rapidly removed and the striatum dissected out on ice. Dopamine (DA), and the metabolites 3,4-dihydroxyphenylacetic acid (DOPAC) and homovanillic acid (HVA) were measured by high-performance liquid chromatography (HPLC) and electrochemical detection. The mobile phase consisted of ($KH_2PO_4$: 0.05 M), octanesulfonic acid (0.4 mM), EDTA (0.1 mM) and methanol (16%) and was adjusted to pH 3 with phosphoric acid, filtered and degassed. The flow rate was 1 ml/min. The HPLC system consisted of a pump (Waters 510) linked to an automatic sample injector (Loop 200 $\mu$l, Waters 717 plus autosampler) and a stainless steel reversed-phase column (Spherisorb ODS2, 5 $\mu$M, 150 × 4.6 mm; Waters, USA) with a pre-column and a coulometric detector (Coulochem II; USA). The working electrode potential was set at 400 mV with a gain of 1 $\mu$A (for dopamine) and 500 nA (for the remaining compounds). The current produced was monitored by means of integration software (Clarity Software, DataApex, Czech Republic).

### *[$^3$H]-WIN 35,428 binding*

[$^3$H]WIN 35428 binding was measured by modification of the method described in detail by Segal et al., (2003) and used as an index of dopamine transporter density. One week after METH administration, the animals were killed and their brains were rapidly removed and the striatum dissected out on ice. Striata were sonicated in ice-cold sodium phosphate buffer (20 mM; pH 7.4) containing sucrose (0.32 M). The homogenate was centrifuged at 30 000 *g* for 15 min at 4 °C. The supernatant was discarded and the wash procedure was repeated twice more. The pellet was finally re-suspended in 60 volumes of homogenization buffer. The assay solution (500 $\mu$l) contained [$^3$H]WIN 35428 (5 nM), desipramine (300 nM) and 100 $\mu$l tissue preparation (approx. 80 $\mu$g protein). Non-specific binding was carried out in the presence of cocaine (30 $\mu$M). The reaction mixture was incubated for 90 min

at 4 °C. The assay was terminated by rapid filtration, and radioactivity was counted by scintillation spectrometry.

### *Immunohistochemistry*

One day after the administration of METH (4 mg/kg, i.p. 3 times, at 3 h intervals), animals were deeply anaesthetized (sodium pentobarbital, 50 mg/kg,) and transcardially perfused with 4% paraformaldehyde. Immunostaining was carried out in free-floating brain sections (30 $\mu$M) with standard avidin–biotin immunohistochemical protocols (Granado et al., 2008), with specific TH antisera (1:1000; Chemicon International, USA) or DAT monoclonal antibody (1:5000; Chemicon International). After incubation with the primary (overnight) and secondary antisera (1 h; Vector Laboratories) peroxidase reactions were developed in diaminobenzidine. For immunofluorescence studies, slices were incubated with rabbit anti- GFAP (1:1000, DakoCytomation, Denmark), rabbit anti-Iba-1 (1:1000, Wako Pure Chemical Industries, Japan); and polyclonal goat anti-IL-15 (1:200, Santa Cruz Biotechnologies, USA), incubated with the corresponding secondary antibodies (AlexaFluor™ 1:1000) and covered with ProLong®Gold (Invitrogen).

Quantification of TH and DAT striatal expression was performed with the aid of an image analysis system (Image J: National Institutes of Health, USA) using a 5× lens. The data are presented as the proportional stained area (total TH- or DAT-positive area/scan area) in the striatal compartments. For immunofluorescence quantification, images taken at 20× lenses were converted to grey scale, and the integrated density within each region of interest for each section was measured with ImageJ. Measurements were carried out in at least 5 animals per treatment (5–6 sections/animal).

### *Fluoro-Jade C staining*

Coronal brain sections (30 $\mu$M) were obtained on a slicing vibratome as described above. The sections were mounted on gelatin-coated slides and allowed to dry fully for 20 min after which they were immersed in 100% ethyl alcohol for 3 min followed by a 1 min soak in 70% alcohol and a 1 min soak in distilled water. The slides were then transferred to a solution of 0.06% potassium permanganate for 15 min. The slides were rinsed for 1 min in distilled water and were then transferred to the Fluoro-Jade staining solution where they were gently agitated for 30 min. The 0.001% working solution of Fluoro-Jade was prepared by adding 10 ml of the stock Fluoro-Jade solution (0.01%) to 90 ml of 0.1% acetic acid in distilled water (Schmued et al., 2005; Granado et al., 2011b). After staining, sections were rinsed 3 times for 1 min each with fresh changes of distilled water. Excess water was drained off. When dry, the slides were immersed in xylene and cover slipped with D.P.X. mounting media (VWR international). Striatal sections were examined with a fluorescence microscope using a filter system suitable for visualizing fluorescein or (FITC). Two different observers counted the Fluoro-Jade positive cells manually.

### *TUNEL histochemistry*

TUNEL histochemistry was carried out *in situ* with the Cell Detection Kit, POD, according to the manufacturer's instructions (Roche, Spain), with minor modifications. In brief, fixed sections were washed and boiled in a microwave for 1 min at 750W in 0.1 M citrate buffer pH=6.0. After blocking with PBS buffer containing 3% BSA and 0.1% Triton X-100, sections were washed and incubated with the TUNEL reaction mixture at 37 °C, washed again and incubated with Converter POD at 37 °C. Next, the sections were washed to remove excess Converter POD, developed with DAB-nickel, covered and analyzed under light microscopy. Positive (DNAse) and negative controls (without TUNEL reaction mixture) were processed in parallel with the experimental groups.

### *Cleaved caspase-3 Western blot*

Mice were killed by cervical dislocation and decapitation 24 h after METH administration, and striata dissected out on ice. Striata were homogenized in buffer containing 50 mM Tris–HCl (pH 7.4), 150 mM NaCl, 1 mM (EGTA), 0.2% NP-40, supplemented with 5% protease and 1% phosphatase inhibitor cocktail (Sigma-Aldrich, USA) and centrifuged at 20 000 *g* for 15 min and the supernatant was collected. Equal amounts of protein (35 $\mu$g) were boiled in laemmli buffer, resolved by 12% sodium dodecyl sulfate polyacrylamide gel electrophoresis (SDS–PAGE) and transferred to polyvinylidene difluoride (PVDF) membranes. Non-specific binding was blocked with TBS buffer containing 0.1% Tween 20 and 5% skimmed milk. Membranes were incubated overnight at 4 °C with anti-cleaved Caspase-3 (Asp175) (Cell Signalling; 1:1000) or anti-$\beta$-actin (Sigma-Aldrich, 1:1000) primary antibodies followed by incubation with donkey anti-rabbit IgG-horseradish peroxidase (Sigma-Aldrich; 1:3000) or goat anti-mouse IgG-horseradish peroxidase (GE Healthcare, Spain; 1:5000) antibodies for 1 h. Each band density was normalized by referring it to its $\beta$-actin band density.

### *Statistics*

Data are presented as mean±standard error of the mean (S.E.M.). All results were analyzed using one-way ANOVA) followed by Newman–Keuls multiple-comparisons test when a significant $F$ value was obtained (GraphPad Prism 5.0, GraphPad Software Inc., USA). Differences were considered significant at $p<0.05$.

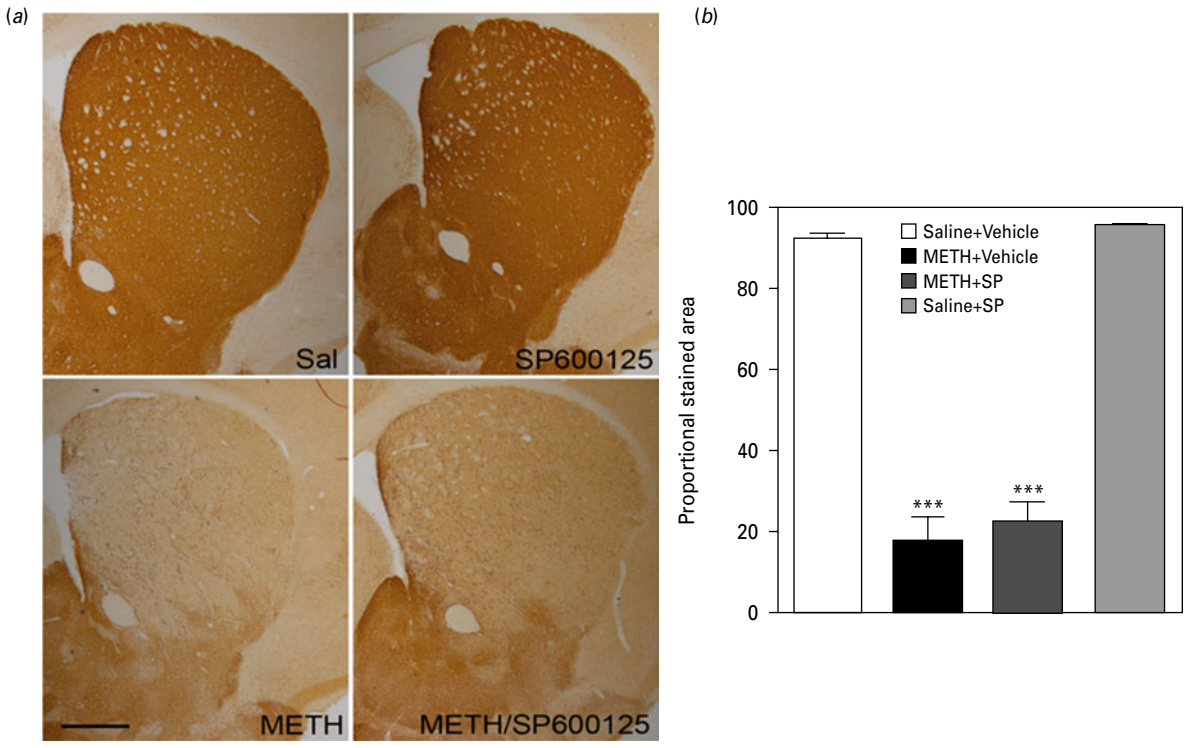


**Fig. 1.** SP600125 (SP, 30 mg/kg i.p.) does not modify the decrease in striatal TH-immunoreactivity induced by METH (4 mg/kg, i.p., 3 times at 3 h intervals). SP600125 was administered 30 min before the last dose of METH. (*a*) Photomicrographs of striatal sections stained for TH from mice 24 h after treatment. (*b*) Histogram shows the proportional stained area of TH immunoreactivity staining in the striatum. Data represent mean ± S.E.M., $n$=5–7 per group. ***$p$<0.001 *vs.* saline, one-way ANOVA followed by Newman–Keuls test. Bar indicates 500 $\mu$M.

## Results

### *METH-induced striatal dopaminergic toxicity is not prevented by SP600125*

Consistent with previous reports (Granado et al., 2011a, b), repeated administration of METH (4 mg/kg, i.p., three times at 3 h intervals) produced dopaminergic axonal neurotoxicity reflected as a marked decrease in the density of TH-ir fibres in striatum 24 h after dosing (Fig. 1*a*). This loss of striatal TH-ir was not modified by the JNK inhibitor SP600125 (30 mg/kg, i.p. 30 min before last METH injection).

Quantitative image analysis by one-way ANOVA revealed a significant effect of treatment (Fig. 1*b*; $F$3,19 = 87.63, $p$<0.0001). *Post-hoc* analysis indicated that METH produced a significant reduction (81%, Fig. 1*b*) in TH-ir that was not altered by co-administration of SP600125 (75%, Fig. 1*b*). SP600125 did not produce any effect in the saline-treated group.

As expected, the pattern of DAT-immunoreactive (DAT-ir) loss produced by METH was very similar to the pattern of TH-ir loss, with a homogeneous decrease in DAT-ir fibres along the rostro-caudal axis and a greater loss of DAT-ir fibres in the lateral parts of the striatum (Fig. 2*a*). This effect was not modified by the JNK inhibitor SP600125.

Quantitative image analysis by one-way ANOVA revealed a significant effect of treatment (Fig. 2*b*; $F$3,19 = 790.9, $p$<0.0001). *Post-hoc* analysis indicated that METH produced a significant reduction (96%, Fig. 2*b*) in DAT-ir that was not altered by co-administration of SP600125 (92%, Fig. 2*b*). SP600125 did not produce any effect in the saline-treated group.

To evaluate the effect of SP600125 on the long-term loss of dopamine nerve terminals induced by METH, we determined the concentration of dopamine and metabolites and the density of dopamine transporters 7 d after METH dosing. One-way ANOVA revealed a significant effect of treatment on dopamine (Fig. 3*a*, $F$3,21 = 89.17, $p$<0.0001), DOPAC (Fig. 3*c*, $F$3,23 = 85.18, $p$<0.0001) and HVA (Fig. 3*d*, $F$3,21 = 69.04, $p$<0.0001) and on dopamine transporter number (Fig. 3*b*, $F$3,15 = 9.38, $p$<0.001). *Post-hoc* analysis indicated that METH reduced all these parameters (77% for DA, 78% for DOPAC, 55% for HVA and 48% for the dopamine transporter), an effect that was not modified by the co-administration of SP600125.

### *SP600125 administration exacerbates METH-induced striatal cell loss*

Fluoro-Jade stains cell bodies, dendrites, and axon terminals of degenerating neurons without staining healthy

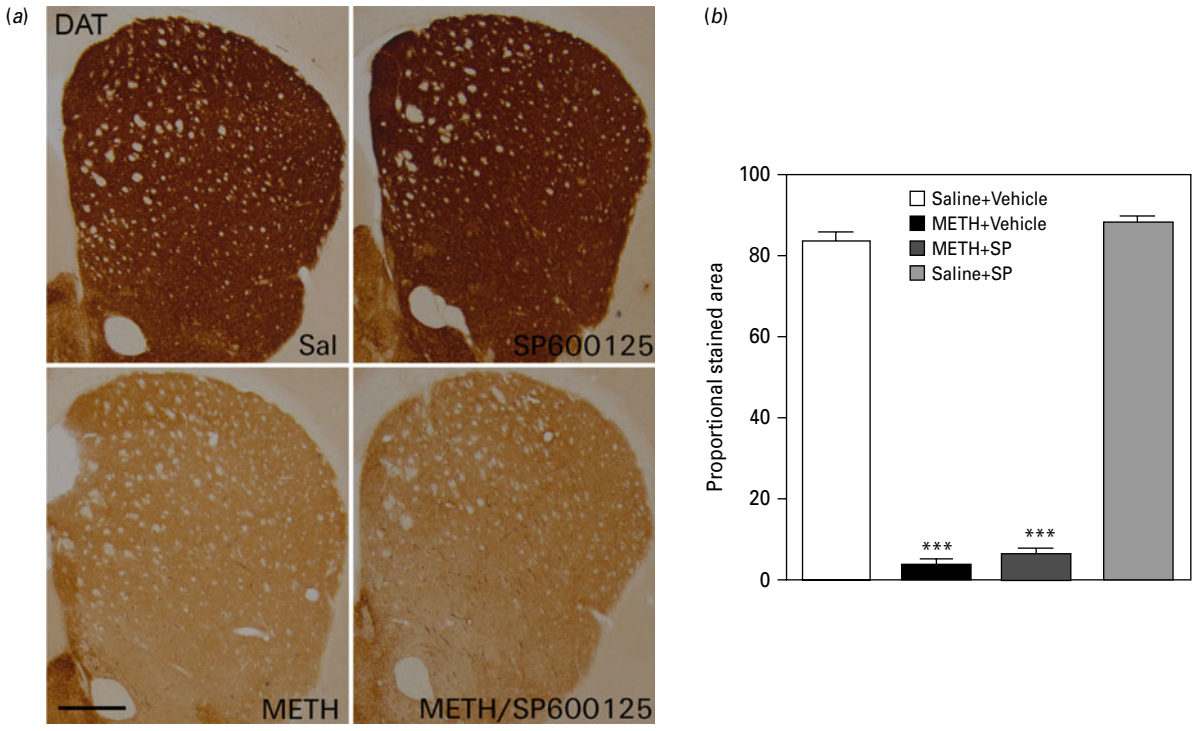


**Fig. 2.** SP600125 (SP, 30 mg/kg, i.p.) does not modify the decrease in striatal DAT-immunoreactivity induced by METH (4 mg/kg, i.p., 3 times at 3 h intervals). SP600125 was administered 30 min before the last dose of METH. (*a*) Photomicrographs of striatal sections stained for DAT from mice 24 h after treatment. (*b*) Histogram shows the proportional stained area of DAT immunoreactivity staining in the striatum. Data represent mean±S.E.M., $n$=5–7 per group. ***$p<0.001$ *vs.* saline, one-way ANOVA followed by Newman–Keuls test. Bar indicates 500 $\mu$M.

neurons (Schmued et al., 2005; Granado et al., 2008, 2011b). Figure 4*a* illustrates a representative image of Fluoro-Jade staining 24 h after METH treatment. One-way ANOVA revealed a significant effect of treatment (Fig. 4*b*; $F3,16=13.65$, $p<0.0001$). *Post-hoc* analysis indicated that METH increased the number of Fluoro-Jade stained cells (159%) in striatum and that this effect was greater in mice treated with METH and SP600125 (353%). SP600125 had no effect in the saline-treated group.

In order to confirm the results obtained with Fluro-Jade staining we determined DNA fragmentation by TUNEL histochemistry and cleaved caspase-3 expression by Western blot. Figure 5*a* illustrates a representative image of TUNEL histochemistry 24 h after METH treatment. One-way ANOVA revealed a significant effect of treatment (Fig. 5*b*; $F3,16=35.64$, $p<0.0001$). *Post-hoc* analysis indicated that METH increased the number of TUNEL positive cells (240%) in striatum and that this effect was greater in mice treated with METH and SP600125 (740%). SP600125 had no effect in the saline-treated group. One of the main executioners of apoptosis is caspase-3 in its activated (cleaved) 17 kDa form. Figure 5*c* shows a representative Western blot of cleaved caspase-3. One-way ANOVA revealed a significant effect of treatment (Fig. 5*d*; $F3,15=8.31$, $p=0.0017$). *Post-hoc* analysis indicated that mice treated with METH and SP600125 showed increased cleaved caspase-3 immunoreactivity (120%) in striatum compared with saline-treated animals and this was significantly greater than that produced by METH alone (50%). SP600125 had no effect in the saline-treated group.

### *SP600125 increases METH-induced glial response*

Glial response has generated great interest, since it is thought to be mediator of amphetamine-like substances neurotoxicity (Thomas et al., 2004a; Yamamoto et al., 2010). We have previously shown that following METH there is an increase in the astroglial and the microglial response. Therefore, we investigated the ability of SP600125 to modify the effect of METH on immunofluorescence staining for GFAP and ionized calcium binding adaptor molecule 1 (Iba-1), markers for astrogliosis and microgliosis, respectively. Figures 6*a* and 7*a* illustrate a representative image of GFAP and Iba-1 staining 24 h after METH treatment.

With respect to the astroglial response, one-way ANOVA revealed a significant effect of treatment (Fig. 6*b*; $F3,16=24.99$, $p<0.0001$). *Post-hoc* analysis indicated that METH increased the number of GFAP staining (130%) in the striatum and that this effect was greater in mice treated with METH and SP600125 (227%). SP600125 had no effect in the saline-treated group.

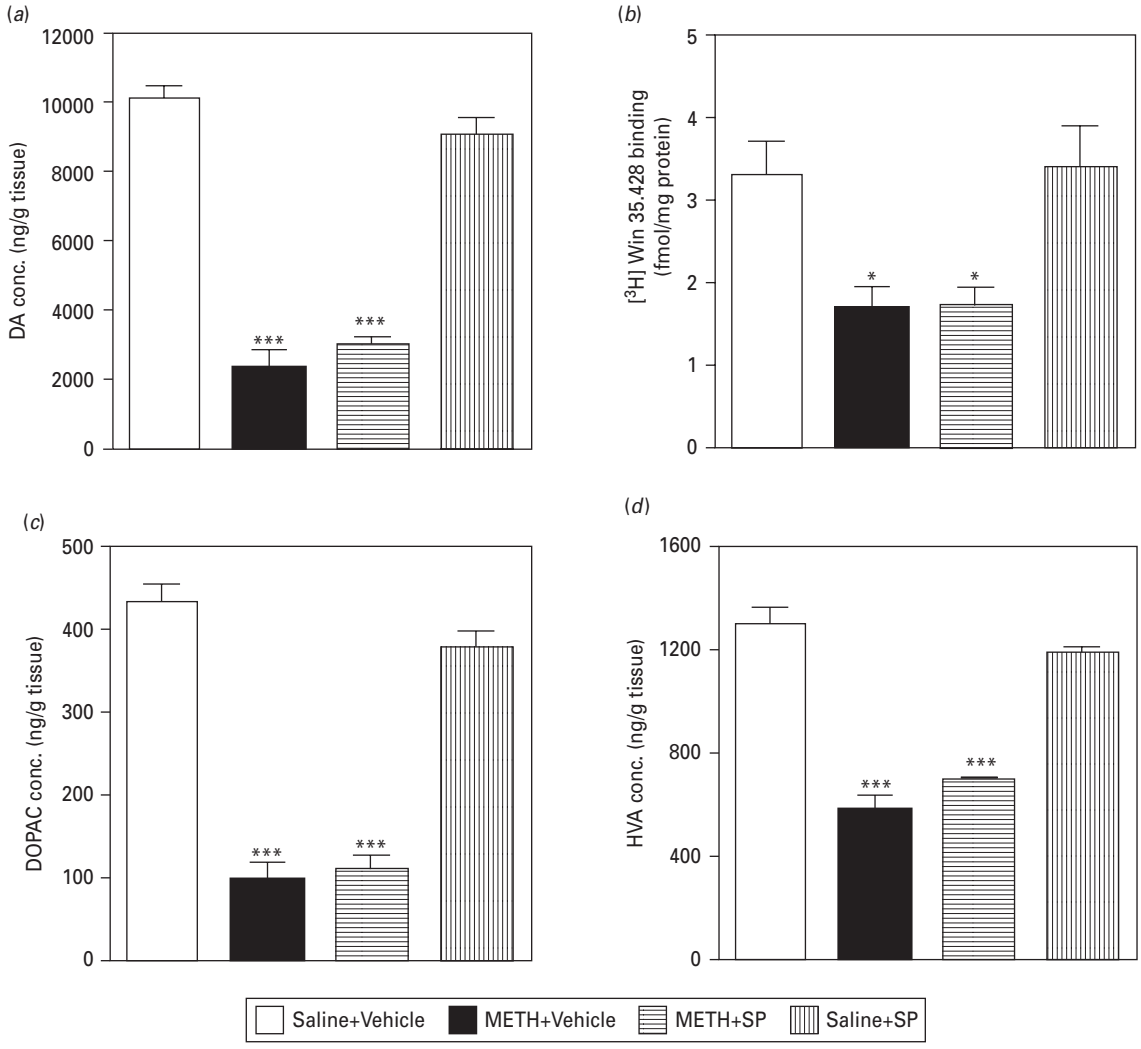


**Fig. 3.** SP600125 (SP, 30 mg/kg i.p.) does not modify the loss of striatal dopamine (*a*), DAT (*b*), DOPAC (*c*) HVA (*d*) induced by METH (4 mg/kg, i.p., 3 times at 3 h intervals) seven days after treatment. SP600125 was administered 30 min before the last dose of METH. Data represent mean±S.E.M., $n$=5–8 per group. *$p<0.05$, ***$p<0.001$ *vs.* saline; one-way ANOVA followed by Newman–Keuls test.

It should be noted that, not only is the number of astrocytes increased, but their shape, indicative of different properties, is also altered becoming more activated as their form turns to a more ameboid phenotype. This effect was more evident in the SP600125+METH group compared with those receiving METH alone. These data indicate that treatment with METH induces enhanced astrogliosis in the presence of the inhibitor of JNK, SP600125.

Regarding Iba-1 immunoreactivity, one-way ANOVA revealed a significant effect of treatment (Fig. 7*b*; $F3,16=12.18$, $p<0.0002$). *Post-hoc* analysis indicated that METH increased the number of Iba-1 staining cells (130%) in striatum and that this effect was greater in mice treated with METH and SP600125 (248%). In this latter group, cells developed into a more activated phenotype reflected by shorter ramifications and an enlarged nucleus (shown in the magnified microphotography). SP600125 had no effect in the saline-treated group.

Taken together, these data demonstrate that inhibition of JNK by SP600125 increased the astrocytic and microglial responses in the striatum of mice treated with METH.

### *SP600125 reduces the METH-induced increase in IL-15 expression*

We also examined the expression of IL-15, an early marker of neuroinflammation (Gómez-Nicola et al., 2008) that we have previously shown to colocalize with GFAP positive cells (Granado et al., 2011b). Figure 8*a* illustrates a representative image of IL-15 24 h after METH treatment. One-way ANOVA revealed a significant effect of treatment (Fig. 8*b* $F3\ 16=5.03$, $p=0.0121$).

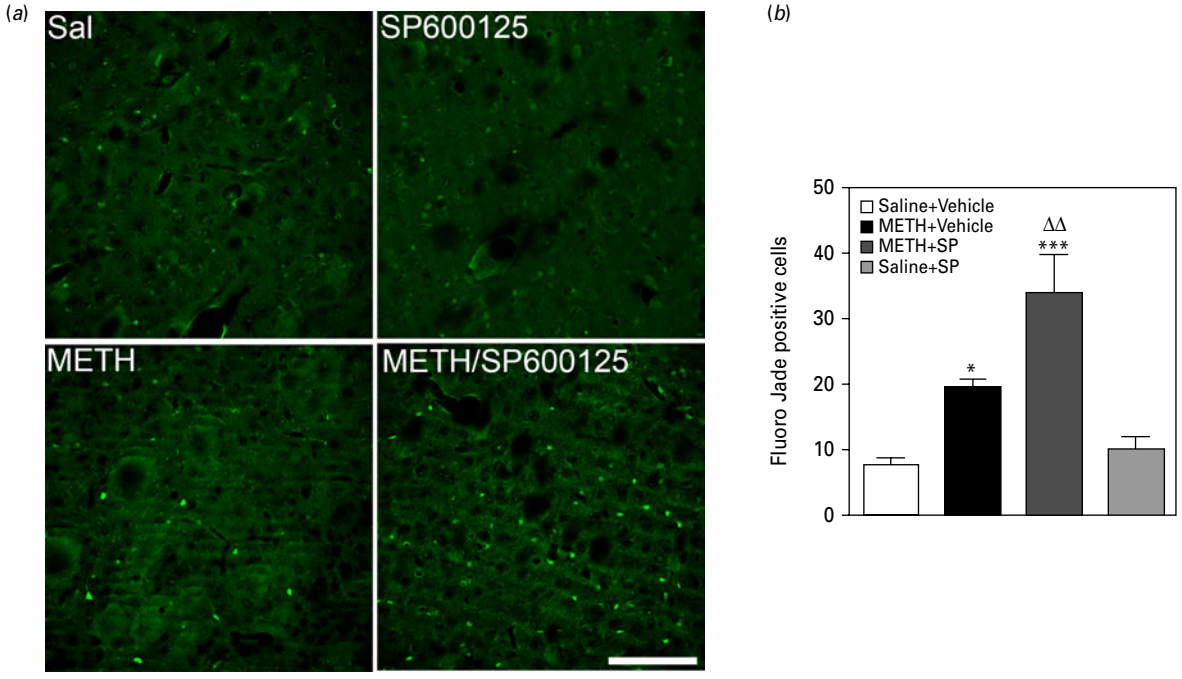


**Fig. 4.** SP600125 (SP, 30 mg/kg i.p.) potentiates the striatal neuron loss induced by METH (4 mg/kg i.p., 3 times at 3 h intervals). SP600125 was administered 30 min before the last dose of METH. (*a*) Photomicrograph of striatal sections stained for Fluoro-Jade from mice 24 h after treatment. (*b*) Histogram shows the number of Fluoro Jade-positive cell bodies. Data represent mean±S.E.M., $n$=4–7 per group. *$p$<0.05, ***$p$<0.001 *vs.* saline; $^{\Delta\Delta}p$<0.01 *vs.* METH-treated group, one-way ANOVA followed by Newman–Keuls test. Bar indicates 100 $\mu$M.

*Post-hoc* analysis indicated that METH increased IL-15 immunoreactivity (23%), an effect that was abolished in mice treated with METH and SP600125. SP600125 alone had no effect in saline-treated mice.

## Discussion

A previous study (Urrutia et al., 2013) showed that repeated administration of METH to mice reduces BBB integrity. One hour after METH treatment there is a reduction in laminin expression and an increase in IgG immunoreactivity and in MMP-9 expression and activity, which colocalizes with areas of greater IgG immunoreactivity. The effect on IgG expression is still evident 24 h after dosing. Injection of the JNK inhibitor, SP600125, 30 min before the last METH administration prevented METH-induced changes in MMP-9 activity, laminin degradation and BBB leakage. SP600125 was also able to prevent the increased p-JNK1/2 expression induced by the drug 1 h after injection. Studies have shown that disruption of BBB is implicated in a large number of neurodegenerative disorders (Zlokovic, 2008). Therefore, the overall aim of the current study was to investigate the effect of the selective JNK1/2 inhibitor SP600125 on the striatal loss of dopamine nerve terminals and on the increased IL-15 expression and glial response induced by METH.

Results reported here confirm that repeated doses of METH induce long-term neurotoxicity and demonstrate that this effect is not prevented by co-administration of SP600125. Seven d after METH injection there is a loss of striatal concentration of dopamine, DOPAC, HVA and density of dopamine transporters, which is similar to that observed in mice receiving METH plus SP600125. The JNK inhibitor not only fails to provide protection against the METH-induced long-term toxicity but also is unable to prevent the reduction in TH- and DAT-ir produced by METH 24 h after dosing. Considering that SP600125 is able to prevent the increased p-JNK1/2 expression induced by METH, results reported in this study indicate that the JNK pathway may not be involved in the striatal dopaminergic neurotoxicity induced by METH.

There are relatively few studies reporting the effect of SP600125 on the dopamine neuronal damage induced by other neurotoxins such as MPTP or 6-OHDA. Results show that SP600125, in addition to reducing MPTP-induced c-Jun phosphorylation, restores the level of TH expression and reduces the loss of TH-positive neurons of SNc (Wang et al., 2004, 2009). It is worth mentioning that in the aforementioned studies, although administered at the same dose as in the current study, SP600125 was injected once daily over 5 consecutive days and coinciding with MPTP injections. However, in our model we were unable to use repeated doses since SP600125 administration 30 min before each of the three METH injections induced a mortality of nearly 80% (data not shown).

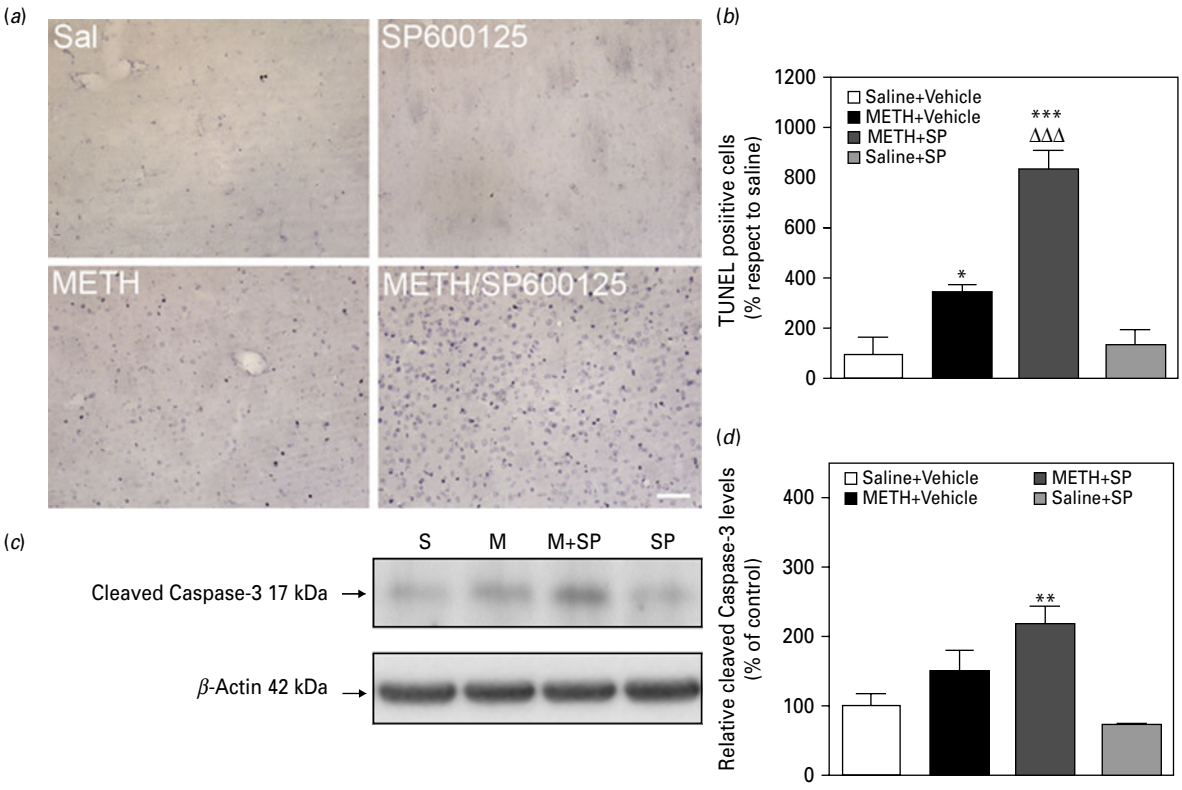


**Fig. 5.** SP600125 (SP, 30 mg/kg i.p.) potentiates the striatal neuronal apoptosis induced by METH (4 mg/kg, i.p., 3 times at 3 h intervals). SP600125 was administered 30 min before the last dose of METH. (*a*) Photomicrograph of striatal sections stained for TUNEL from mice 24 h after treatment. Bar indicates 100 $\mu$M. (*b*) Histogram shows the number of TUNEL positive cells. Data represent mean±S.E.M., $n$=4–6 per group. (*c*) Representative Western blots showing immunoreactivity of cleaved caspase-3 and (*d*) Quantitative analysis of protein expression relative to $\beta$-actin. Data represent mean±S.E.M. $n$=3–6. *$p$<0.05, **$p$<0.01, ***$p$<0.001 *vs.* saline; $^{\Delta}p$<0.05, $^{\Delta\Delta\Delta}p$<0.001 *vs.* METH-treated group, one-way ANOVA followed by Newman–Keuls test.

It is clear that JNK plays a role in neurodegeneration, specifically in models of Parkinson disease, and is a putative therapeutic target for preventing neuronal death. However, the JNK pathway does not appear to participate in axonal degeneration (Ries et al., 2008) so other therapeutic targets will need to be identified to halt that component of the degenerative process. There is now substantial evidence that the molecular pathways underlying destruction of the cell soma are separate and distinct from those, which mediate destruction of axons (Raff et al., 2002; Coleman, 2005).

It is also relevant to consider that the down-stream factors involved in MPTP damage are not the same as those in METH damage. It has been described that COX2 is a molecular target of JNK activation in mesencephalon and it is essential for MPTP-induced dopaminergic cell death (Hunot et al., 2004). Our results show that following METH there is no change in the striatal expression of COX2 (Supplementary Figure S1).

In recent years it has been demonstrated that apart from classical monoaminergic toxicity, METH induces non-monoaminergic neuronal soma degeneration in the striatum of rodents (Jayanthi et al., 2004, 2005; Zhu et al., 2009). The affected cells have been identified as the GABAergic neurons expressing enkephalin and parvalbumin (Jayanthi et al., 2005; Thiriet et al., 2005). Supporting these observations, and as previously reported (Granado et al., 2011b), repeated METH administration resulted in the appearance of Fluoro-Jade positive immunostaining in striatum, a marker of degenerating neurons (Schmued et al., 2005). Interestingly, not only did SP600125 fail to prevent the striatal cell loss induced by METH, it increased the number of Fluoro-Jade and TUNEL positive cells and the cleavage of caspase-3 supporting a survival role of JNK pathway activation in METH-induced striatal neuronal degeneration.

In line with this, data in the literature indicate that the JNK pathway also participates in the regulation of cell proliferation, survival and differentiation (Davis, 2000) suggesting that JNK also carries out physiological functions, substantial levels of JNK expression and activity can be detected in the striatum of untreated mice (ElAli et al., 2012; Urrutia et al., 2013). Several factors appear to be involved in the different consequences of JNK activation including the intensity or duration of a signal with transient JNK activation promoting cell survival and prolonged JNK activation inducing cellular apoptosis (Ventura et al., 2006). In the current study following

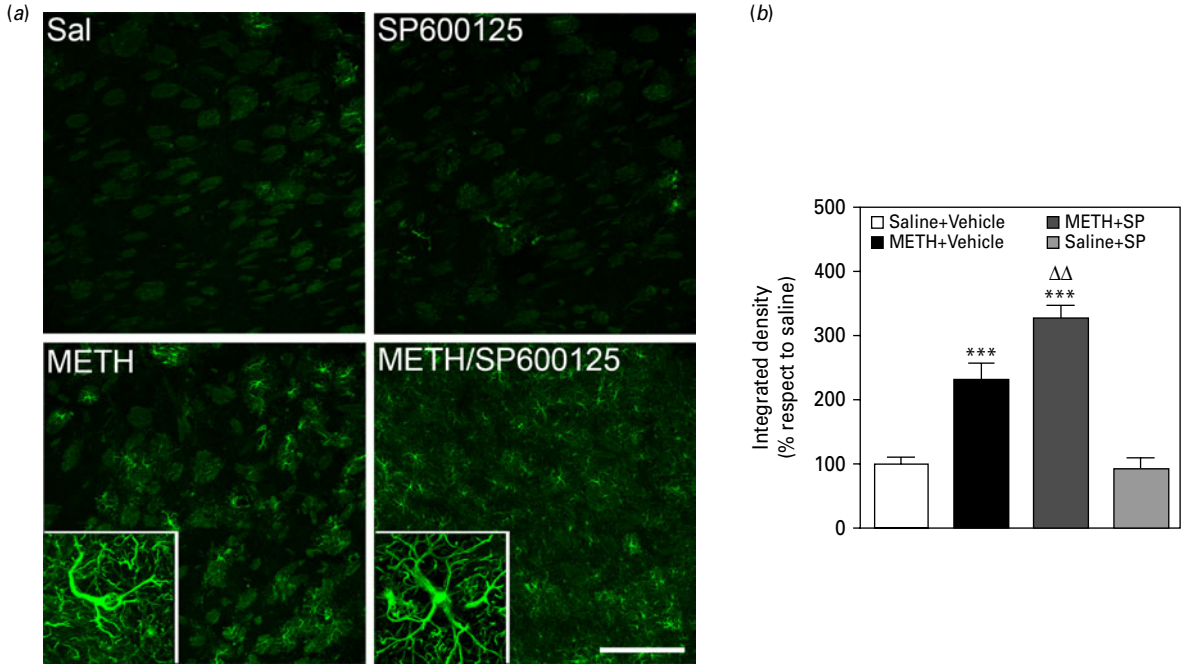


**Fig. 6.** SP600125 (SP, 30 mg/kg i.p.) potentiates astrogliosis induced by METH (4 mg/kg, i.p., 3 times at 3 h intervals). SP600125 was administered 30 min before the last dose of METH. (*a*) Photomicrographs of striatal sections stained with GFAP from mice 24 h after treatment. (*b*) Histogram shows the integrated density of GFAP immunoreactivity staining. Data represent mean ± S.E.M., $n=4$–7 per group. ***$p<0.001$ *vs.* saline, $^{\Delta\Delta}p<0.01$ *vs.* METH-treated group; one-way ANOVA followed by Newman–Keuls test. Bar indicates 200 $\mu$M.

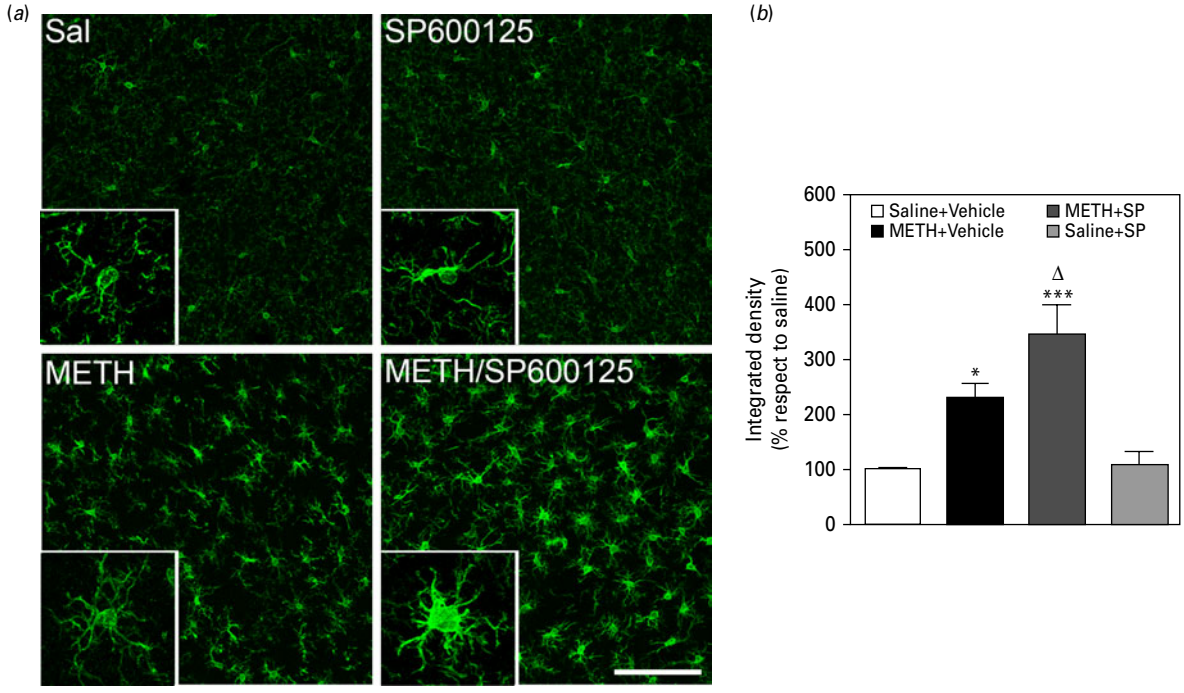


**Fig. 7.** SP600125 (SP, 30 mg/kg i.p.) potentiates microgliosis induced by METH (4 mg/kg i.p., 3 times at 3 h intervals). SP600125 was administered 30 min before the last dose of METH. (*a*) Photomicrographs of striatal sections stained with Iba-1 from mice 24 h after treatment. (*b*) Histogram shows the integrated density of Iba-1 immunoreactivity staining. Data represent mean ± S.E.M., $n=5$–7 per group. *$p<0.05$, ***$p<0.001$ *vs.* saline, $^{\Delta}p<0.05$ *vs.* METH-treated group; one-way ANOVA followed by Newman–Keuls test. Bar indicates 100 $\mu$M.

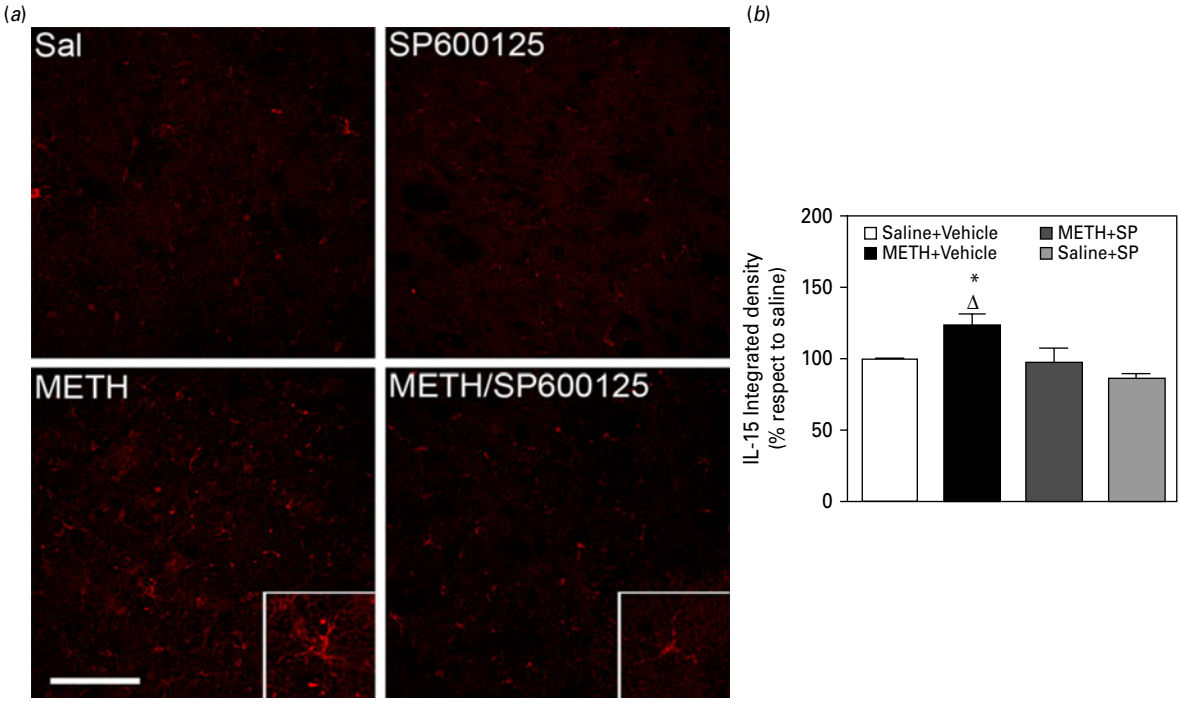


**Fig. 8.** SP600125 (SP, 30 mg/kg i.p.) attenuates the increase in IL-15 expression induced by METH (4 mg/kg, i.p., 3 times, at 3 h intervals). SP600125 was administered 30 min before the last dose of METH. (*a*) Photomicrographs of striatal sections stained for IL-15 from mice 24 h after treatment. (*b*) Histogram shows the integrated density of IL-15 immunoreactivity staining. Data represent mean ± S.E.M., $n$=4–6 per group. *$p$<0.05 *vs.* saline, $^{\Delta}p$<0.05 *vs.* METH-treated group; one-way ANOVA followed by Newman–Keuls test. Bar indicates 100 $\mu$M.

METH there was a robust but transient increase in JNK1/2 phosphorylation in total brain lysates 1 h (Urrutia et al., 2013) and 3 h (ElAli et al., 2012) after METH administration, which disappeared within 24 h of METH exposure.

In line with a deleterious effect of JNK1/2 inhibition, our results show that SP600125 increases the glial response induced by METH. GFAP staining is considered to be a hallmark of neurotoxicity and has been closely associated with METH or MDMA-induced striatal dopaminergic neurotoxicity (Fornai et al., 2004; Busceti et al., 2008; Granado et al., 2011b; Ares-Santos et al., 2012). Genetic inactivation of dopamine D1 or D2 receptors prevents astrogliosis and provides protection against the neurotoxic effects of METH (Granado et al., 2011a; Ares-Santos et al., 2012). Microglial activation has also been strongly associated with METH-induced dopaminergic neurodegeneration in the striatum of mice (LaVoie et al., 2004; Thomas et al., 2004a, b; Yamamoto et al., 2010), and is considered another marker for amphetamine neurotoxicity (Thomas et al., 2004b). In response to neuronal injury, microglia develop into an activated phenotype, characterized by a more ameboid-like shaped cell, changes that are proportional to the magnitude of the injury (Kreutzberg, 1996; Raivich et al., 1999). Activated microglia could then be involved in METH-induced neurotoxicity through the release of pro-inflammatory cytokines and reactive oxygen and nitrogen species which could potentiate neuronal injury. On the other hand, minocycline administration attenuated microglial activation but failed to protect from METH-induced dopaminergic neurotoxicity in mice striatum (Sriram et al., 2006). In contrast, the radical scavenger edaravone protected dopaminergic terminals without affecting METH-induced microglial activation (Kawasaki et al., 2006). Regardless of whether or not glial activation is directly related to METH-induced dopaminergic neurotoxicity, our data show a strong relationship between gliosis and the number of Fluoro-Jade positive cells, suggesting a potential role of reactive microglia/astroglia in METH-induced neuronal damage.

Very little is known about the regulation and role of IL-15 in the brain. In a previous paper (Granado et al., 2011b) we reported that METH-induced expression of IL-15 was localized in astrocytes but not in microglia. As SP600125 enhanced the METH-induced glial response, we expected an increase in IL-15 immunoreactivity compared with METH-injected animals. In contrast, we observed that administration of SP600125 interfered with the METH-induced increase in IL-15 immunoreactivity in the mouse striatum, pointing to regulation of the expression of this pleiotropic cytokine by the JNK pathway. Interestingly, these same animals with reduced IL-15 expression showed greater neurodegeneration suggesting a protective role for this protein, in line with some recent data reporting enhanced severity of

experimental autoimmune encephalomyelitis in IL-15 knockout mice (Wu et al., 2010).

Our data indicate that, SP600125 a JNK inhibitor, does not protect against the dopaminergic damage induced by METH and, in fact, potentiates the glial response and the striatal cell body loss caused by the drug. Therefore, considering the dual effects of JNK activation more studies are required to clarify the putative role of JNK as a therapeutic target for preventing neuronal death.

## Supplementary material

For supplementary material accompanying this paper, visit http://dx.doi.org/10.1017/S1461145713000850

## Acknowledgments

This work was supported by grants from the Spanish Ministerio de Economia y Competitivad (MINECO), Ministerio de Sanidad, Servicios Sociales e Igualdad, ISCIII and Universidad Complutense-Comunidad de Madrid: SAF2010-21529; PNSD PR47/10-17826, PR61/08-16410, RedRTA (RD06/0001/0006; RD12/0028/0002), FIS PI070892 and UCM-CAM 910258. AU and NG were involved in the conception, design, acquisition, analysis and interpretation of data. MDGL and RM were involved in the interpretation of data. EOS and MIC were involved in drafting the article, critical discussion of results and final approval of the version to be published.

## Statement of interest

None.

## References

Ares-Santos S, Granado N, Oliva I, O'Shea E, Martin ED, Colado MI, Moratalla R (2012) Dopamine D(1) receptor deletion strongly reduces neurotoxic effects of methamphetamine. Neurobiol Dis 45:810–820.

Borsello T, Clarke PG, Hirt L, Vercelli A, Repici M, Schorderet DF, Bogousslavsky J, Bonny C (2003) A peptide inhibitor of c-Jun *N*-terminal kinase protects against excitotoxicity and cerebral ischemia. Nat Med 9:1180–1186.

Busceti CL, Biagioni F, Riozzi B, Battaglia G, Storto M, Cinque C, Molinaro G, Gradini R, Caricasole A, Canudas AM, Bruno V, Nicoletti F, Fornai F (2008) Enhanced tau phosphorylation in the hippocampus of mice treated with 3,4-methylenedioxymethamphetamine ("Ecstasy"). J Neurosci 28:3234–3245.

Coleman M (2005) Axon degeneration mechanisms: commonality amid diversity. Nat Rev Neurosci 6:889–898.

Davis RJ (2000) Signal transduction by the JNK group of MAP kinases. Cell 103:239–252.

Deng X, Cadet JL (1999) Methamphetamine administration causes overexpression of nNOS in the mouse striatum. Brain Res 851:254–257.

Deng X, Jayanthi S, Ladenheim B, Krasnova IN, Cadet JL (2002) Mice with partial deficiency of c-Jun show attenuation of methamphetamine-induced neuronal apoptosis. Mol Pharmacol 62:993–1000.

ElAli A, Urrutia A, Rubio-Araiz A, Hernandez-Jimenez M, Colado MI, Doeppner TR, Hermann DM (2012) Apolipoprotein-E controls adenosine triphosphate-binding cassette transporters ABCB1 and ABCC1 on cerebral microvessels after methamphetamine intoxication. Stroke 43:1647–1653.

Fornai F, Lenzi P, Gesi M, Soldani P, Ferrucci M, Lazzeri G, Capobianco L, Battaglia G, De Blasi A, Nicoletti F, Paparelli A (2004) Methamphetamine produces neuronal inclusions in the nigrostriatal system and in PC12 cells. J Neurochem 88:114–123.

Gómez-Nicola D, Valle-Argos B, Suardíaz M, Taylor JS, Nieto-Sampedro M (2008) Role of IL-15 in spinal cord and sciatic nerve after chronic constriction injury: regulation of macrophage and T-cell infiltration. J Neurochem 107:1741–1752.

Granado N, O'Shea E, Bove J, Vila M, Colado MI, Moratalla R (2008) Persistent MDMA-induced dopaminergic neurotoxicity in the striatum and substantia nigra of mice. J Neurochem 107:1102–1112.

Granado N, Ares-Santos S, O'Shea E, Vicario-Abejón C, Colado MI, Moratalla R (2010) Selective vulnerability in striosomes and in the nigrostriatal dopaminergic pathway after methamphetamine administration : early loss of TH in striosomes after methamphetamine. Neurotox Res 18:48–58.

Granado N, Ares-Santos S, Oliva I, O'Shea E, Martin ED, Colado MI, Moratalla R (2011a) Dopamine D2-receptor knockout mice are protected against dopaminergic neurotoxicity induced by methamphetamine or MDMA. Neurobiol Dis 42:391–403.

Granado N, Lastres-Becker I, Ares-Santos S, Oliva I, Martin E, Cuadrado A, Moratalla R (2011b) Nrf2 deficiency potentiates methamphetamine-induced dopaminergic axonal damage and gliosis in the striatum. Glia 59:1850–1863.

Hirata H, Cadet JL (1997) p53-knockout mice are protected against the long-term effects of methamphetamine on dopaminergic terminals and cell bodies. J Neurochem 69:780–790.

Hogan KA, Staal RG, Sonsalla PK (2000) Analysis of VMAT2 binding after methamphetamine or MPTP treatment: disparity between homogenates and vesicle preparations. J Neurochem 74:2217–2220.

Hunot S, Vila M, Teismann P, Davis RJ, Hirsch EC, Przedborski S, Rakic P, Flavell RA (2004) JNK-mediated induction of cyclooxygenase 2 is required for neurodegeneration in a mouse model of Parkinson's disease. Proc Natl Acad Sci USA 101:665–670.

Imam SZ, Newport GD, Itzhak Y, Cadet JL, Islam F, Slikker W, Ali SF (2001) Peroxynitrite plays a role in methamphetamine-induced dopaminergic neurotoxicity: evidence from mice lacking neuronal nitric oxide synthase gene or overexpressing copper-zinc superoxide dismutase. J Neurochem 76:745–749.

Itzhak Y, Gandia C, Huang PL, Ali SF (1998) Resistance of neuronal nitric oxide synthase-deficient mice to methamphetamine-induced dopaminergic neurotoxicity. J Pharmacol Exp Ther 284:1040–1047.

Itzhak Y, Martin JL, Ail SF (2000) nNOS inhibitors attenuate methamphetamine-induced dopaminergic neurotoxicity but not hyperthermia in mice. Neuroreport 11:2943–2946.

Jayanthi S, Deng X, Noailles PA, Ladenheim B, Cadet JL (2004) Methamphetamine induces neuronal apoptosis via cross-talks between endoplasmic reticulum and mitochondria-dependent death cascades. FASEB J 18:238–251.

Jayanthi S, Deng X, Ladenheim B, McCoy MT, Cluster A, Cai NS, Cadet JL (2005) Calcineurin/NFAT-induced up-regulation of the Fas ligand/Fas death pathway is involved in methamphetamine-induced neuronal apoptosis. Proc Natl Acad Sci USA 102:868–873.

Kawasaki T, Ishihara K, Ago Y, Nakamura S, Itoh S, Baba A, Matsuda T (2006) Protective effect of the radical scavenger edaravone against methamphetamine-induced dopaminergic neurotoxicity in mouse striatum. Eur J Pharmacol 542:92–99.

Krasnova IN, Cadet JL (2009) Methamphetamine toxicity and messengers of death. Brain Res Rev 60:379–407.

Kreutzberg GW (1996) Microglia: a sensor for pathological events in the CNS. Trends Neurosci 19:312–318.

LaVoie MJ, Card JP, Hastings TG (2004) Microglial activation precedes dopamine terminal pathology in methamphetamine-induced neurotoxicity. Exp Neurol 187:47–57.

Morishima Y, Gotoh Y, Zieg J, Barrett T, Takano H, Flavell R, Davis RJ, Shirasaki Y, Greenberg ME (2001) Beta-amyloid induces neuronal apoptosis via a mechanism that involves the c-Jun *N*-terminal kinase pathway and the induction of Fas ligand. J Neurosci 21:7551–7560.

O'Callaghan JP, Miller DB (1994) Neurotoxicity profiles of substituted amphetamines in the C57BL/6J mouse. J Pharmacol Exp Ther 270:741–751.

Raff MC, Whitmore AV, Finn JT (2002) Axonal self-destruction and neurodegeneration. Science 296:868–871.

Raivich G, Bohatschek M, Kloss CU, Werner A, Jones LL, Kreutzberg GW (1999) Neuroglial activation repertoire in the injured brain: graded response, molecular mechanisms and cues to physiological function. Brain Res Brain Res Rev 30:77–105.

Repici M, Chen X, Morel MP, Doulazmi M, Sclip A, Cannaya V, Veglianese P, Kraftsik R, Mariani J, Borsello T, Dusart I (2012) Specific inhibition of the JNK pathway promotes locomotor recovery and neuroprotection after mouse spinal cord injury. Neurobiol Dis 46:710–721.

Ries V, Silva RM, Oo TF, Cheng HC, Rzhetskaya M, Kholodilov N, Flavell RA, Kuan CY, Rakic P, Burke RE (2008) JNK2 and JNK3 combined are essential for apoptosis in dopamine neurons of the substantia nigra, but are not required for axon degeneration. J Neurochem 107:1578–1588.

Sanchez V, Zeini M, Camarero J, O'Shea E, Bosca L, Green AR, Colado MI (2003) The nNOS inhibitor, AR-R17477AR, prevents the loss of NF68 immunoreactivity induced by methamphetamine in the mouse striatum. J Neurochem 85:515–524.

Saporito MS, Brown EM, Miller MS, Carswell S (1999) CEP-1347/KT-7515, an inhibitor of c-jun *N*-terminal kinase activation, attenuates the 1-methyl-4-phenyl tetrahydropyridine-mediated loss of nigrostriatal dopaminergic neurons *in vivo*. J Pharmacol Exp Ther 288:421–427.

Schmued LC, Stowers CC, Scallet AC, Xu L (2005) Fluoro-Jade C results in ultra high resolution and contrast labeling of degenerating neurons. Brain Res 1035:24–31.

Segal DS, Kuczenski R, O'Neil ML, Melega WP, Cho AK (2003) Escalating dose methamphetamine pretreatment alters the behavioral and neurochemical profiles associated with exposure to a high-dose methamphetamine binge. Neuropsychopharmacology 28:1730–1740.

Sonsalla PK, Nicklas WJ, Heikkila RE (1989) Role for excitatory amino acids in methamphetamine-induced nigrostriatal dopaminergic toxicity. Science 243:398–400.

Sriram K, Miller DB, O'Callaghan JP (2006) Minocycline attenuates microglial activation but fails to mitigate striatal dopaminergic neurotoxicity: role of tumor necrosis factor-alpha. J Neurochem 96:706–718.

Thiriet N, Deng X, Solinas M, Ladenheim B, Curtis W, Goldberg SR, Palmiter RD, Cadet JL (2005) Neuropeptide Y protects against methamphetamine-induced neuronal apoptosis in the mouse striatum. J Neurosci 25:5273–5279.

Thomas DM, Walker PD, Benjamins JA, Geddes TJ, Kuhn DM (2004a) Methamphetamine neurotoxicity in dopamine nerve endings of the striatum is associated with microglial activation. J Pharmacol Exp Ther 311:1–7.

Thomas DM, Dowgiert J, Geddes TJ, Francescutti-Verbeem D, Liu X, Kuhn DM (2004b) Microglial activation is a pharmacologically specific marker for the neurotoxic amphetamines. Neurosci Lett 367:349–354.

Thomas DM, Francescutti-Verbeem DM, Kuhn DM (2008) The newly synthesized pool of dopamine determines the severity of methamphetamine-induced neurotoxicity. J Neurochem 105:605–616.

UNODC (2012) World Drug Report. United Nations publication, Sales No. E.12.X1.1.

Urrutia A, Rubio-Araiz A, Gutierrez-Lopez MD, ElAli A, Hermann DM, O'Shea E, Colado MI (2013) A study on the effect of JNK inhibitor, SP600125, on the disruption of blood-brain barrier induced by methamphetamine. Neurobiol Dis 50:49–58.

Ventura JJ, Hübner A, Zhang C, Flavell RA, Shokat KM, Davis RJ (2006) Chemical genetic analysis of the time course of signal transduction by JNK. Mol Cell 21:701–710.

Wang W, Shi L, Xie Y, Ma C, Li W, Su X, Huang S, Chen R, Zhu Z, Mao Z, Han Y, Li M (2004) SP600125, a new JNK inhibitor, protects dopaminergic neurons in the MPTP model of Parkinson's disease. Neurosci Res 48:195–202.

Wang Y, Zhang Y, Wei Z, Li H, Zhou H, Zhang Z (2009) JNK inhibitor protects dopaminergic neurons by reducing COX-2 expression in the MPTP mouse model of subacute Parkinson's disease. J Neurol Sci 285:172–177.

Wu X, Pan W, He Y, Hsuchou H, Kastin AJ (2010) Cerebral interleukin-15 shows upregulation and beneficial effects in experimental autoimmune encephalomyelitis. J Neuroimmunol 223:65–72.

Yamamoto BK, Moszczynska A, Gudelsky GA (2010) Amphetamine toxicities: classical and emerging mechanisms. Ann N Y Acad Sci 1187:101–121.

Zhu J, Xu W, Wang J, Ali SF, Angulo JA (2009) The neurokinin-1 receptor modulates the methamphetamine-induced striatal apoptosis and nitric oxide formation in mice. J Neurochem 111:656–668.

Zlokovic BV (2008) The blood-brain barrier in health and chronic neurodegenerative disorders. Neuron 57:178–201.